Electromagnetically induced transparency in an open Λ-type molecular lithium system

A. Lazoudis,[1] T. Kirova,[1] E. H. Ahmed,[1,*] L. Li,[2] J. Qi,[3] and A. M. Lyyra[1]
[1]*Department of Physics, Temple University, Philadelphia, Pennsylvania 19122-6082, USA*
[2]*Department of Physics, Tsinghua University, Beijing 100084, China*
[3]*Department of Physics and Astronomy, Pennsylvania State University, Berks Campus, Reading, Pennsylvania 19610, USA*
(Received 7 April 2010; published 20 August 2010)

We present an experimental study of electromagnetically induced transparency (EIT) in a Λ-type molecular lithium system. Copropagating beam geometry is utilized in order to minimize the residual Doppler width. A coupling laser power dependent study of the EIT feature is carried out. Our findings have been complemented by theoretical studies of open systems that trace the presence of EIT starting from the density-matrix equations. Numerical simulations have been performed and are in good agreement with the experimental results.

DOI: 10.1103/PhysRevA.82.023812 PACS number(s): 42.50.Gy, 42.50.Hz, 33.40.+f

I. INTRODUCTION

There has been considerable interest in the phenomenon of electromagnetically induced transparency (EIT) [1] due to its wide range of possible applications in quantum optics. A widely used energy-level scheme for the study of EIT is the Λ-type system consisting of two ground-state levels coupled by two laser fields to a common excited-state level. In this scheme, the transition between the two lower states is not dipole allowed. Such an energy-level scheme was employed for the first time by Alzetta *et al.* [2] in their experimental discovery of coherent population trapping (CPT) in atoms. Two years later, CPT was observed by Gray *et al.* [3] in a similar Λ-type system. Since then, many experiments have been performed in systems with a Λ-level configuration, including the first experimental demonstration of EIT [4].

The closely related to EIT phenomenon of "slow light" [5] was experimentally observed in ultracold sodium gas [6] and strontium vapor [1]. Fleischhauer and Lukin proposed an effective "light-storage" technique via "dark-state polaritons" [7] to trap, store, and recover light on demand. The storage and consequent retrieval of light pulses using this scheme have been implemented in different types of media, including Bose-Einstein condensates (BECs) [8], thermal gases [9], and solids [10,11]. Cheng and Han [12] showed that it is possible to achieve single-mode slow light propagation, which is advantageous over the multimode operation, while Hansen and Mølmer [13] proved theoretically the benefits of trapping of light via standing-wave EIT in media consisting of stationary atoms (e.g., ultracold gases or solids). Light-storage techniques based on EIT are becoming more popular since they are relatively easy to implement and facilitate the practical realization of all-optical quantum information processing and quantum computation.

The superluminal light propagation [14] in an EIT medium has also attracted considerable attention due to its potential applications in data processing, optoelectronics, communications, and networking. Negative group velocity [15] as well as the controllable sign of dispersion were reported in Cs vapor [16].

Multilevel schemes, including additional levels, such as Y [17,18], inverted-Y [19,20], N [21,22], and tripod types [23] in atomic systems have recently drawn attention in the study of light storage [24], which gives new prospects for their use as multi-channel quantum memory units.

The coupling of the same level with two strong fields leads to a multipeak pattern understood in the light of doubly dressed states [25,26].

Driving a hyperfine transition within the ground state in a Λ-type system by an rf field [27] leads to splitting of the EIT resonance into a doublet. Double EIT features due to doubly dressed states are also observed in a cascade-type Cs atom [28]. The EIT position changes with the detuning of the pump field. In this work, the role of Doppler broadening is also studied and shown to lead to a light shift of the center frequencies of both peaks.

Progress is also made in incorporating inhomogeneous Doppler broadening [29–32] and the open character [33] of the actual experimental systems to the homogeneously broadened closed three-level schemes [34,35], usually used as theoretical models of EIT in atomic systems.

In addition, EIT is finding new applications in Doppler cooling [36], generating entanglement between spatially separated atomic BECs [37] and nanoscale-resolution fluorescence microscopy [38].

As interesting as EIT and its associated phenomena and applications are, systematic investigations of EIT in molecules are still lacking. To our knowledge, there are only a handful of theoretical and experimental studies of EIT in molecular systems.

Zhou *et al.* [39] studied theoretically EIT in a Λ-type polar molecular system. The model was build for the HCN molecule and showed that the existence of permanent dipole moments is detrimental in the common $1+1$ photon process due to induced oscillations. However, in the $2+2$ photon case, which is not observed in atoms and nonpolar molecules, the presence of permanent dipole moments leads to perfect EIT conditions, gain without inversion, and the possibility to controllably reverse the two processes by choosing the right permanent dipole moment ratio.

In addition, the effect of incoherent pumping on the width of EIT was investigated in a model LiH Λ system [40] in the cases of both homogeneous and inhomogeneous broadening.

*erahmed@temple.edu

Experimentally, EIT was observed in cascade-type Doppler-broadened Li_2 [41], K_2 [42], and Na_2 [43,44] in vapor phase, V type in Na_2 vapor [45], Λ type in acetylene molecules in a hollow-core photonic gap fiber [46], Λ and V scheme in acetylene photonic microcell [47], and Λ type in Cs_2 vapor [48].

The main difficulties in working with molecules originate in their much smaller transition-dipole-moment matrix elements [49–51] compared to those in atoms, as well as the existence of multiple decay channels to energy levels that are not involved in the main excitation scheme.

In this work, we investigate EIT both theoretically and experimentally in an open Λ-type molecular lithium system at high temperatures; therefore, the system experiences inhomogeneous line broadening. The detailed description of experimental setup and measurements are given in Sec. II.

It is worth noting that, as in our previous work [41–45], we detected the presence of EIT as a dip in the fluorescence spectrum rather than in the absorption of the probe field. The equivalence of the two methods is shown in [52–54]. Some authors [53] point out the advantages of using fluorescence detection since it allows avoiding additional effects such as stimulated emission of Raman signals.

Our theoretical analysis takes into account various broadening mechanisms, for example, Doppler broadening, transit decay rate of the molecules out of the laser beams, and spontaneous decay to levels not coupled in the excitation scheme. The theoretical model is developed for an open three-level molecular system. Under the steady-state conditions, we solve the density-matrix equations using perturbation theory and obtain analytical expressions for the matrix elements. In Sec. VI, we compare the numerically calculated results with the experimental measurements.

II. EXPERIMENTS

For our experiments, we have chosen the Li_2 molecule, since it has been very well characterized. The selected energy-level configuration for molecular lithium is sketched in Fig. 1. The levels $|1\rangle$ and $|3\rangle$ are rovibrational levels of the ground electronic state ($X^1\Sigma_g^+$), while level $|2\rangle$ is a rovibrational level from the first excited singlet electronic state ($A^1\Sigma_u^+$). The structures of the electronic states $X^1\Sigma_g^+$ and $A^1\Sigma_u^+$ [55–60] are very well known. A coupling laser was tuned to the $X^1\Sigma_g^+$ ($v'' = 0$, $J'' = 12$) → $A^1\Sigma_u^+$ ($v' = 5$, $J' = 13$) transition, exciting molecules from ground state $|3\rangle$ to the upper state $|2\rangle$, while the probe laser was scanned around the $X^1\Sigma_g^+$ ($v'' = 1$, $J'' = 14$) → $A^1\Sigma_u^+$ ($v' = 5$, $J' = 13$) transition. A five-arm stainless-steel heat-pipe oven [61], with argon buffer gas, was used to generate lithium molecules in gas phase. Lithium heat pipe typically is operated at pressures of the buffer gas at 1 Torr or above. At such pressures, collisional transfer effects in the excited states can be observed [62]. In order to avoid them, we chose to work at lower pressure in the 260–320 mTorr range, where we did not observe any collisional satellite lines to the main ones in fluorescence. This indicates that in our experiments collisions do not affect in a significant way the population of the upper state. From the Doppler line width of one laser excitation, as given in Fig. 2, it was estimated

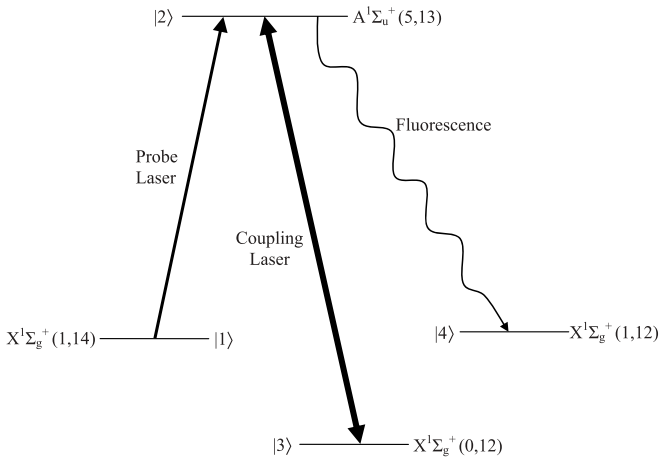

FIG. 1. Li_2 energy-level configuration. In this Λ-excitation scheme, the probe is tuned to the $X^1\Sigma_g^+$ (1,14) → $A^1\Sigma_u^+$ (5,13) transition while the coupling laser is on resonance with the $X^1\Sigma_g^+$ (0,12) → $A^1\Sigma_u^+$ (5,13) transition. The resonance laser frequencies for the probe and coupling transitions are 14850.793 and 15231.778 cm^{-1}, respectively. The fluorescence signal is detected at the 14887 cm^{-1} window that corresponds to the decay of molecules from the upper state $A^1\Sigma_u^+$ (5,13) to the ground state $X^1\Sigma_g^+$ (1,12). The ground-state levels noted as $|1\rangle$, $|3\rangle$, and $|4\rangle$ are different vibrational levels of the same electronic state. The Frank-Condon factors of the coupling and probe field transitions are 0.113 and 0.068, respectively.

that the temperature of the vapor is about 820 K. The ends of the heat-pipe arms were water cooled in order to protect the heat-pipe windows from the alkali vapor.

The probe and coupling laser beams were produced by two tunable continuous wave (cw) ring dye lasers (Coherent 699–29 autoscan, line width 0.5 MHz) operating with DCM (4-dicyanomethylene-2-methyl-6-p-dimethylaminostyryl-4H-pyran) dye. Both dye lasers were pumped by a single argon ion laser (Coherent Innova 100–20). The two laser beams were linearly polarized in the vertical

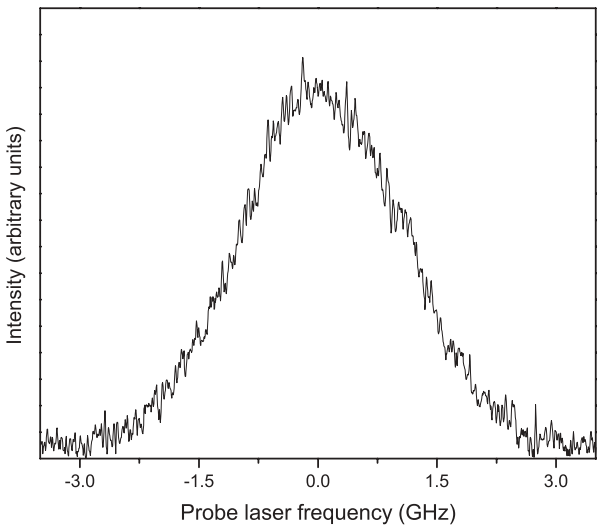

FIG. 2. Doppler-broadened fluorescence spectrum of Li_2 $A^1\Sigma_u^+$ (5,13) → $X^1\Sigma_g^+$ (1,12) transition. The Doppler width is approximately 2.44 GHz.

direction and copropagated coaxially through the heat-pipe oven. All laser frequencies were calibrated by using standard iodine reference spectra [63,64]. The intensity of the coupling field was varied by using a metal-coated neutral-density filter. In order to ensure that the probe field propagates within the spatial profile of the coupling field, the spot size of the probe beam (diameter at $1/e^2$ of 160 μm) was made smaller than that of the coupling beam (diameter at $1/e^2$ of 475 μm). To reduce the transit-time effect, the probe laser was focused to a radius that corresponded to a transit relaxation rate of about two orders of magnitude less that the decay rates of the excited states [65]. Through the course of our experiments, the spatial profile of each laser beam was measured using the knife-edge method [66,67].

The population of the upper level $|2\rangle$ was monitored by detecting the fluorescence from this level to a specific rovibrational level of the ground state using a double monochromator (SPEX 1404) as a narrow-band filter. Due to selection rules, the upper state can decay only to levels of the ground electronic state with rotational quantum numbers of $J' \pm 1$. The monochromator was set at 148 87 cm^{-1} to detect the fluorescence signal corresponding to the R-branch transition $A\,^1\Sigma_u^+$ $(v' = 5, J' = 13) \rightarrow X\,^1\Sigma_g^+$ $(v'' = 1, J'' = 12)$. The monohromator isolated the fluorescence of this transition from all the other decay transitions. Its resolution is of the order of 0.5 cm^{-1}, while the closest transition to the monitored one is the P-branch transition $A\,^1\Sigma_u^+$ $(v' = 5, J' = 13) \rightarrow X\,^1\Sigma_g^+$ $(v'' = 1, J'' = 14)$ at 148 51 cm^{-1}. As a detector, a Peltier cooled photomultiplier tube (PMT; Hamamatsu, R928) was used. The signal from the PMT was amplified with a lock-in amplifier (SRS 850) and was recorded as a function of the probe laser frequency.

III. DENSITY-MATRIX EQUATIONS OF MOTION

In order to interpret the experimental results and describe the dynamics of our open system, we employ the density-matrix formalism. The Hamiltonian of a three-level system under the rotating-wave approximation in the interaction picture is given by

$$\hat{H} = \hbar\Omega_1\left(|1\rangle\langle 2| + |2\rangle\langle 1|\right) + \hbar\Delta_1|2\rangle\langle 2| + \hbar\Omega_2\left(|2\rangle\langle 3| + |3\rangle\langle 2|\right) + \hbar\left(\Delta_1 + \Delta_2\right)|3\rangle\langle 3|. \quad (1)$$

Here, $\Omega_1 = \frac{\mu_{21}E_1}{2\hbar}$ is the half-Rabi frequency of the probe laser with amplitude E_1 and $\Omega_2 = \frac{\mu_{23}E_2}{2\hbar}$ is the half-Rabi frequency of the coupling laser with amplitude E_2.

The laser detunings are defined for the homogeneously broadened case:

$$\Delta_1 = \omega_{21} - \omega_1, \quad (2a)$$

$$\Delta_2 = \omega_2 - \omega_{23}. \quad (2b)$$

The density-matrix equation reads

$$\frac{d\rho_I}{dt} = -\frac{i}{\hbar}[H_I, \rho_I] + \text{relaxation terms}. \quad (3)$$

In a molecular system, the decay phenomena are extremely complicated compared with those of atoms. It is a challenge to theoretically model such systems. The difficulty in modeling open systems is associated with the existence of many decay channels between molecular states. For molecules in excited rovibrational energy states, there are numerous pathways of decay to lower vibration-rotation levels. To account for the decay of the excited state out of the coupled ground levels, we model all other ground-state levels as a single level $|4\rangle$ (Fig. 3). In order to account for the additional relaxation of each state due to the molecules traversing through the laser beams for a finite time, we introduce the transit rate w_t.

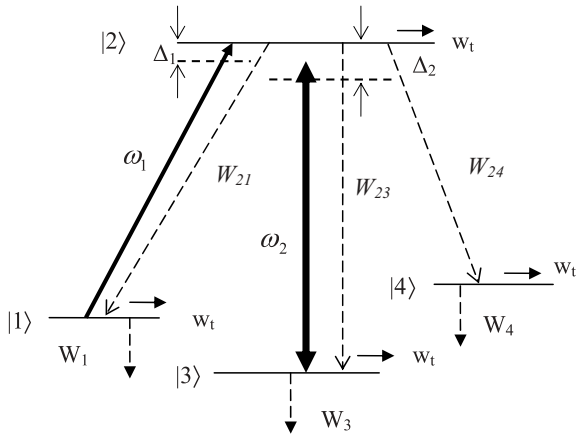

FIG. 3. Relaxation processes in an open four-level Λ-type system. All the rovibrational levels of the ground $X\,^1\Sigma_g^+$ electronic states other than $|1\rangle$ and $|3\rangle$ to which decay from level $|2\rangle$ is possible are treated as a single level, $|4\rangle$. Ω_1 and Ω_2 are the Rabi frequencies of the probe and coupling fields, respectively. Here, W_{ij} denotes the population decay from level $|\text{i}\rangle$ to level $|\text{j}\rangle$, W_i indicates the natural decay rate of state $|\text{i}\rangle$, and w_t is the transit rate. Note that since the ground-state levels $|1\rangle$, $|3\rangle$, and $|4\rangle$ are long-lived states, their decay rates will be much smaller than w_t and W_2. The detunings of the probe and coupling fields are Δ_1 and Δ_2, respectively.

In the experiment, only continuous-wave (CW) lasers were used, thus a steady-state approximation in Eq. (3) can be made $(d\rho_I/dt = 0)$. The individual components of Eq. (3) for our system have the following form:

$$W_1^t\rho_{11} - i\Omega_1\left(\rho_{12} - \rho_{21}\right) - W_{21}\rho_{22} = W_1^t\rho_{11}^e, \quad (4a)$$

$$i\Omega_1(\rho_{11} - \rho_{22}) + \left(i\Delta_1 - \gamma_{12}^t\right)\rho_{12} + i\Omega_2\rho_{13} = 0, \quad (4b)$$

$$i\Omega_2\rho_{12} + \left[i\left(\Delta_1 + \Delta_2\right) - \gamma_{13}^t\right]\rho_{13} - i\Omega_1\rho_{23} = 0, \quad (4c)$$

$$i\Omega_1(\rho_{22} - \rho_{11}) - \left(i\Delta_1 + \gamma_{12}^t\right)\rho_{21} - i\Omega_2\rho_{31} = 0, \quad (4d)$$

$$i\Omega_1\left(\rho_{12} - \rho_{21}\right) + i\Omega_2\left(\rho_{32} - \rho_{23}\right) + W_2^t\rho_{22} = 0, \quad (4e)$$

$$-i\Omega_1\rho_{13} + i\Omega_2(\rho_{22} - \rho_{33}) + \left(i\Delta_2 - \gamma_{23}^t\right)\rho_{23} = 0, \quad (4f)$$

$$-i\Omega_2\rho_{21} - \left[i\left(\Delta_1 + \Delta_2\right) + \gamma_{31}^t\right]\rho_{31} + i\Omega_1\rho_{32} = 0, \quad (4g)$$

$$i\Omega_1\rho_{31} + i\Omega_2\left(\rho_{33} - \rho_{22}\right) - \left(i\Delta_2 + \gamma_{32}^t\right)\rho_{32} = 0, \quad (4h)$$

$$-W_{23}\rho_{22} - i\Omega_2\left(\rho_{32} - \rho_{23}\right) + W_3^t\rho_{33} = W_3^t\rho_{33}^e, \quad (4i)$$

$$-W_{24}\rho_{22} + W_4^t\rho_{44} = W_4^t\rho_{44}^e. \quad (4j)$$

For simplicity in the notation, we have introduced W_i^t and γ_{ij}^t defined as $W_i^t = W_i + w_t$ and $\gamma_{ij}^t = \gamma_{ij} + w_t$. W_i is the decay rate of level i, while W_{ij} indicates the spontaneous emission rate of level i to j and ρ_{ii}^e is the population of level $|i\rangle$ at thermal

equilibrium. The damping rate, γ_{ij}, is given by

$$\gamma_{nm} = \gamma_{mn} = \frac{1}{2}\sum_k (W_{ik} + W_{jk}) + \gamma_{ij}^{\text{col}}, \tag{5}$$

where γ_{ij}^{col} is the collision dephasing rate.

IV. ANALYTICAL EXPRESSIONS IN THE WEAK PROBE LIMIT

When the probe laser is much weaker than the coupling laser ($\Omega_1 \ll \Omega_2$), the system of equations (4) can be solved explicitly [68,69]. Initially, in the absence of the probe field, the population of ground level $|3\rangle$ is optically pumped by the coupling field to level $|2\rangle$. By setting $\Omega_1 = 0$ in (4), we obtain the zeroth-order solution for the system

$$\rho_{11}^{(0)} = \rho_{11}^{e} + \frac{\rho_{33}^{e}}{F}\left(\frac{W_{21}}{W_1^t}\right), \tag{6a}$$

$$\rho_{22}^{(0)} = \frac{\rho_{33}^{e}}{F}, \tag{6b}$$

$$\rho_{33}^{(0)} = \left(\frac{1}{F}\frac{W_{23} - W_2^t}{W_3^t} + 1\right)\rho_{33}^{e}, \tag{6c}$$

$$\rho_{32}^{(0)} = \frac{i\Omega_2}{\gamma_{23}^t + i\Delta_2}\left[\frac{1}{F}\left(\frac{W_{23} - W_2^t}{W_3^t} - 1\right) + 1\right]\rho_{33}^{e}, \tag{6d}$$

where

$$F = 1 - \frac{W_{23} - W_2^t}{W_3^t} + \frac{W_2^t\left(\gamma_{32}^{t^2} + \Delta_2^2\right)}{2\Omega_2^2\gamma_{32}^t}, \tag{7}$$

When the weak perturbation is turned on (probe field), the population of the upper state is modified. Then, the density-matrix element ρ_{22}, to the second order in the probe laser Rabi frequency, becomes

$$\rho_{22}^{(2)} = -\frac{i\Omega_1}{W_2^t}\left(\rho_{12}^{(1)} - \rho_{21}^{(1)}\right) - \frac{i\Omega_2}{W_2^t}\left(\rho_{32}^{(2)} - \rho_{23}^{(2)}\right), \tag{8}$$

while the first-order solution for the coherence ρ_{12} is obtained as

$$\rho_{12}^{(1)} = \frac{i\Omega_1\left(\gamma_{13}^t - i\Delta_1 - i\Delta_2\right)}{\left(-\gamma_{12}^t + i\Delta_1\right)\left(\gamma_{13}^t - i\Delta_1 - i\Delta_2\right) - \Omega_2^2} \times\left[\left(2 + \frac{W_{24}}{W_4^t}\right)\rho_{22}^{(0)} + \rho_{33}^{(0)} + \rho_{44}^{e} - 1 + \frac{i\Omega_2}{\gamma_{13}^t - i\Delta_1 - i\Delta_2}\rho_{23}^{(0)}\right]. \tag{9}$$

The absorption of the probe is determined by the imaginary part of the density-matrix element ρ_{12} while the real part leads to the dispersion profile of the probe transition. The resonance structure of ρ_{12} is determined by the singularities arising from the term $1/(-\gamma_{12}^t + i\Delta_1)(\gamma_{13}^t - i\Delta_1 - i\Delta_2) - \Omega_2^2$. The roots of the denominator of this expression are

$$\Delta_{1,\pm} = -\frac{\Delta_2}{2} \pm \frac{1}{2}\sqrt{4\Omega_2^2 + \Delta_2^2 - \left(\gamma_{13}^t - \gamma_{12}^t\right)^2 + 2i\left(\gamma_{13}^t - \gamma_{12}^t\right)\Delta_2} - i\frac{\gamma_{13}^t + \gamma_{12}^t}{2}. \tag{10}$$

When Ω_2 is much larger than γ_{ij} and Δ_2, Eq. (10) simplifies to $\Delta_{1\pm} = \pm\Omega_2$. The absorption line as function of the probe-laser detuning Δ_1 splits into two peaks (Autler-Townes doublet) [70] of equal amplitude, positioned at $\pm\Omega_2$.

The population of level $|2\rangle$, given by Eq. (8), is monitored by the experimentally detected fluorescence signal. Moreover, the upper-level population spectrum has similar characteristics with the absorption line shape of the probe transition. It has been shown for a closed [52] and open V system [45] that the absorption profile is directly proportional to the population of the upper level. Furthermore, for a closed Λ or an open cascade system, density-matrix analysis has revealed [71,72] a linear dependence between the absorption and fluorescence signals.

V. EFFECTS OF DOPPLER BROADENING AND MAGNETIC SUBLEVEL DEGENERACY

So far in our analysis, we have considered the homogeneously broadened case. Since our experiments are performed in a Doppler-broadened regime, the response of the three-level system must include contributions from all molecular-velocity groups.

In the Doppler-broadened Λ system with two copropagating laser beams, the detunings of the probe and coupling fields are given by

$$\delta_1(\upsilon_z) = \Delta_1 - k_1\upsilon_z, \tag{11a}$$

$$\delta_2(\upsilon_z) = \Delta_2 - k_2\upsilon_z, \tag{11b}$$

where k_1 and k_2 are the corresponding wave numbers.

The velocity distribution of the molecules is assumed to be a Maxwellian according to

$$N(\upsilon_z) = \frac{N_o}{u_p\sqrt{\pi}}\exp\left(-\frac{\upsilon_z^2}{u_p^2}\right), \tag{12}$$

where N_o is the molecular density and $u_p = (2kT/m)^{\frac{1}{2}}$ is the most probable velocity of a molecule. The contribution of all molecular velocities is obtained by integrating the density-matrix elements over the distribution $N(\upsilon_z)$:

$$\langle\rho_{ij}\rangle_{\text{Doppler}} = \int_{-\infty}^{\infty}\rho_{ij}(\upsilon_z)N(\upsilon_z)d\upsilon_z. \tag{13}$$

Each rotational band in high-resolution spectra of diatomic molecules with angular momentum J is composed of $2J + 1$ discrete lines, corresponding to the magnetic sublevels M_J of the particular transition, which represent the projection of J on the direction of the external laser E field.

The Rabi frequency of a $(v'',J'') \rightarrow (v',J')$ transition depends on the magnetic quantum number M_J of the states involved [73] according to

$$\Omega_{i,M} = \frac{\mu_{el}|\langle v''|v'\rangle|E_i}{\hbar} f, \tag{14}$$

where f is the rotational strength factor originating from the M_J-dependent transition dipole moment, E_i is the amplitude of the applied field, and $\mu_{\rm el}$ is the electronic transition dipole moment. The rotational strength factor f depends on the molecular electronic transitions (P, Q, and R transitions respectively) and the field polarizations. Specifically, for $^1\Sigma^+ \rightarrow {}^1\Sigma^+$ electronic transitions, the rotational strength factors f induced by a linearly polarized laser field are [74]

$$f_R = \sqrt{\frac{(J+1)^2 - M_J^2}{(2J+1)(2J+3)}}, \text{ for an R transition,} \tag{15a}$$

and

$$f_P = \sqrt{\frac{J^2 - M_J^2}{(2J+1)(2J-1)}}, \text{ for a P transition.} \tag{15b}$$

Since each Rabi frequency is a function of the magnetic number M_J, an average over all magnetic sublevels is required [75]. This can be expressed mathematically by summing Eq. (13) over all M_J values, leading to the final expression for the density-matrix element ρ_{ij}

$$\langle \rho_{ij} \rangle_{M_J,\text{Doppler}} = \sum_{M_J} \int_{-\infty}^{\infty} \rho_{ij}(v_z) N(v_z) dv_z. \tag{16}$$

In an inhomogeneously broadened medium and for low coupling-field intensities, the splitting of the M_J levels is masked under the Doppler effect. The M_J-dependent AT splitting has been demonstrated in a lithium molecule in a sub-Doppler broadening condition [76].

VI. SIMULATIONS OF EXPERIMENTAL DATA AND DISCUSSION

In a Doppler-broadened environment, it is possible to observe EIT even when the available coupling laser power is unable to produce an Autler-Townes splitting larger than the Doppler width. In this case, the condition to be satisfied is that the Autler-Townes splitting, which is essentially equal to the Rabi frequency of the coupling field, must exceed the residual Doppler line width of the two-photon resonance transition [54,77]. For a three-level system with a Λ- or V-type energy-level configuration, the residual Doppler line width is expressed by

$$\Delta v_D = |\vec{k_1} - \vec{k_2}|v, \tag{17}$$

where v is the most probable molecular velocity and k_1, k_2 are the wave numbers of the probe and coupling lasers, respectively. The wave numbers $\vec{k_i}$ take a positive value when the laser propagates along the $+z$ axis and negative when the propagation is in the opposite direction. Unlike demonstration of EIT in the cold atoms case [78] or in the atomic beam case [79], where the Doppler effect is eliminated, in thermal sample one must select the proper beam geometry in order to minimize Δv_D. It is clear from Eq. (17) that the EIT feature is more likely to be resolved when the two laser beams copropagate in the heat-pipe oven. Moreover, the residual Doppler line width can be further reduced if both laser fields have similar wavelengths.

Application of a strong coupling field to our system (Fig. 1), in the absence of a probe field, results in the splitting of the upper level $|2\rangle$ into two components (Autler-Townes doublet). Now, as the weak probe field is tuned near resonance, these Autler-Townes components interfere destructively and the system experiences a strong reduction at the line center of the absorption profile. It is the quantum interference between the two states that gives rise to EIT [17]. The transparency of the medium to the propagating probe laser is caused by the two effects working in tandem. Thus, both the Autler-Townes effect and destructive interference contribute to the value of absorption. The amount of contribution of each effect depends on the properties of the medium and the applied fields. In fact, an analysis on a closed three-level Λ-type system has shown [69] that quantum interference is dominant in the weak-probe regime, while in the regime where the strength of the probe field increases sufficiently both effects become equally important.

It is well known that in three-level Λ-type systems, EIT takes place when the frequencies of the probe and coupling laser satisfy the two-photon Raman condition [34]:

$$\Delta_1 + \Delta_2 = 0. \tag{18}$$

Thus, the location of the EIT resonance is independent of the molecular transitions and the relative powers of the fields but shifts with the detuning of the coupling beam in agreement with Eq. (18). Therefore, it is not necessary to have both fields resonant with the optical transitions in order to observe a transparency window.

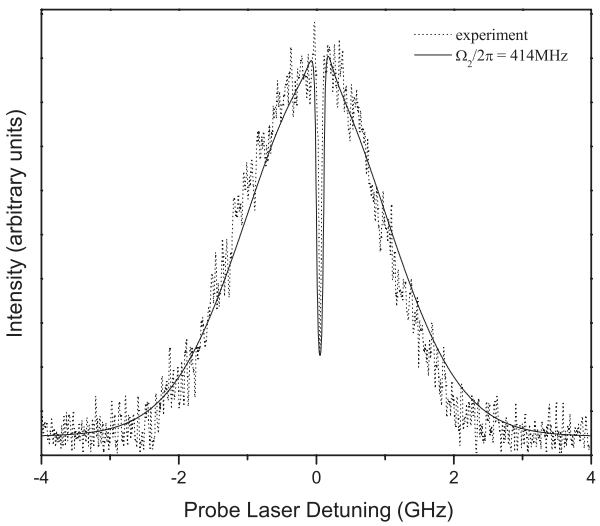

FIG. 4. Simulated experimental data. The fluorescence of $|2\rangle \rightarrow |1\rangle$ as a function of the probe laser detuning is simulated. The coupling Rabi frequency is 414 MHz. The probe Rabi frequency is 25 MHz. For a better fit, the coupling field detuning is set to -55 MHz. All collisional dephasing rates are estimated to be $\gamma_{ij}^{\rm col}/2\pi = 4$ MHz, while the transit decay rate is calculated as $w_t/2\pi = 0.47$ MHz.

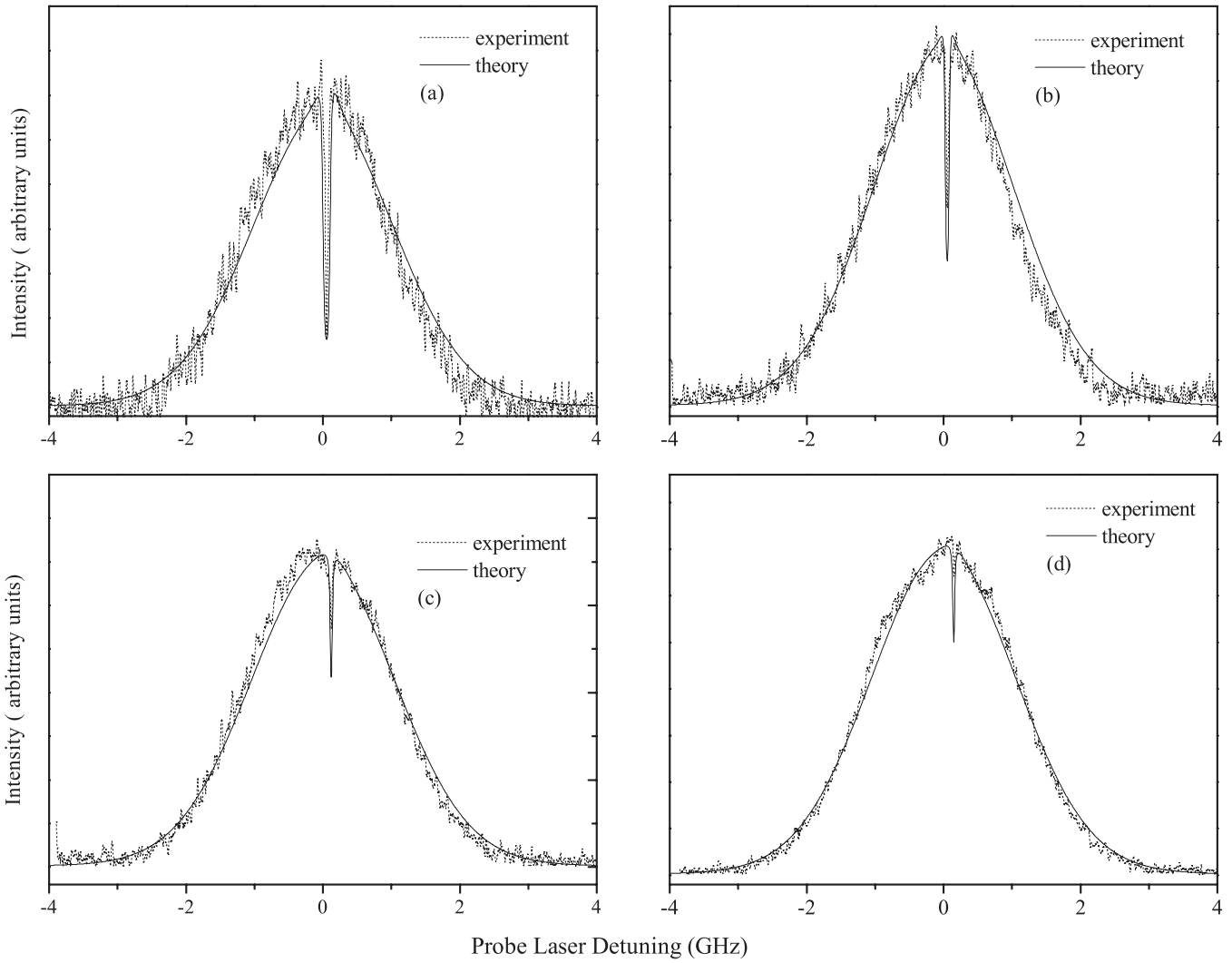

FIG. 5. Fluorescence signal for different coupling field powers. Probe laser scan detected via $A\,^1\Sigma_u^+$ (5,13) $\rightarrow$ $X\,^1\Sigma_g^+$ (1,12) fluorescence signal with coupling field power (a) 407 mW ($\Omega_2/2\pi = 414$ MHz), (b) 118 mW ($\Omega_2/2\pi = 223$ MHz), (c) 24 mW ($\Omega_2/2\pi = 100$ MHz), and (d) 6 mW ($\Omega_2/2\pi = 50$ MHz). The probe laser power was kept at 5 mW. For a better fit, the coupling field detuning is set to (a), (b) -55 MHz, (c) -124 MHz, and (d) -152 MHz.

In order to compare our theoretical model with the experimental data, we calculate numerically the population of the upper level $|2\rangle$ for the Li_2 system. In our evaluation, we use the experimentally estimated values of all the relevant parameters. The lifetimes of the ground-state levels $|1\rangle$, $|3\rangle$, and $|4\rangle$ were assumed to be of the order of 10^{-3} sec [80]. The natural lifetime of the excited state $|2\rangle$ for the Li_2 system has been measured to be 18.8 ns [81]. However, after including collisional redistribution, we use a value of 17 ns in our simulations. The Rabi frequency associated with the coupling field was calculated by employing the appropriate spot size, laser field intensity, and M_J-dependent transition dipole moment $\mu_{i,i+1}^{M_J}$ [76]. Using the experimentally measured electronic transition dipole moment $\mu_e(R)$ for the $A\,^1\Sigma_u^+ - X\,^1\Sigma_g^+$ transition of Li_2 [51], and LEVEL 7.5 program [82], we calculated the transition-dipole-moment matrix element for the $X\,^1\Sigma_g^+$ $(v'' = 0,\ J'' = 12) \rightarrow A\,^1\Sigma_u^+$ $(v' = 5, J' = 13)$ to be 2.7984 Debye.

After performing a series of numerical calculations, we notice, as predicted by the theory, that the depth of the dip at line center is sensitive to the choice of the dephasing rates γ_{ij}. Since we are unable to make a reliable measurement of the collisional dephasing rates $\gamma_{ij}^{\rm col}$, we select those values that approximately reproduce the experimental EIT spectrum. For that purpose, all collisional dephasing rates were given the value $\gamma_{ij}^{\rm col}/2\pi = 4$ MHz. In addition, the broadening caused by the molecules entering and exiting the interaction region is $w_t/2\pi = 0.47$ MHz [65].

Without the coupling field, scanning of the probe laser across the $|1\rangle \rightarrow |2\rangle$ transition yielded the normal Doppler-broadened fluorescence spectrum, as shown in Fig. 2. When we turn on the strong coupling laser, a dip at the center of the Doppler-broadened fluorescence spectrum emerges, which indicates that the population of molecules in the upper state has been greatly reduced (Fig. 4). Our numerical simulations are in good agreement with the recorded data, as illustrated in Fig. 4. The depth of the EIT dip fits well, while its width is overrepresented by the simulation. The small discrepancy between the simulated and experimentally observed width of

the EIT dip is mainly due to the lack of precise knowledge of the collisional processes in the system. The observed EIT effect is strongly dependent on the coupling Rabi frequency as illustrated in Fig. 5, where a series of the fluorescence spectra versus the probe laser detuning for different power values of the coupling laser are shown. The power of the coupling field was attenuated via a neutral density filter to 6 mW. The experimental results displayed in Fig. 5 show strong reductions in the fluorescence signal for increasing coupling laser intensity.

VII. CONCLUSIONS

In our work, we investigated EIT both theoretically and experimentally in an open Λ-type molecular system. The experiments were carried out in gas-phase inhomogeneously broadened lithium dimer samples. We propose a theoretical model by using the density-matrix formalism that takes into account various broadening mechanisms, as well as the openness of the molecular system. In the limit of a weak probe field, perturbation theory solutions are derived, leading to an in-depth description of the physical processes of EIT in open systems. Finally, inclusion of inhomogeneous Doppler broadening and magnetic sublevel degeneracy in our theoretical model allowed for a good comparison between numerical calculations and experimental measurements.

ACKNOWLEDGMENTS

We gratefully acknowledge valuable discussions with L. M. Narducci and T. Abi-Salloum and financial support from National Science Foundation Grants No. PHY 0216187, No. PHY 0555608, and No. PHY 0855502.

[1] S. E. Harris, Phys. Today **50**, 36 (1997).
[2] G. Alzetta, A. Gozzini, L. Moi, and G. Orriols, Nuovo Cimento **36**, 5 (1976).
[3] H. R. Gray, R. M. Whitley, and C. R. Stroud Jr., Opt. Lett. **3**, 218 (1978).
[4] K. J. Boller, A. Imamoglu, and S. E. Harris, Phys. Rev. Lett. **66**, 2593 (1991).
[5] S. E. Harris, J. E. Field, and A. Kasapi, Phys. Rev. A **46**, R29 (1992).
[6] L. V. Hau, S. E. Harris, Z. Dutton, and C. H. Behroozi, Nature (London) **397**, 594 (1999).
[7] M. Fleischhauer and M. D. Lukin, Phys. Rev. Lett. **84**, 5094 (2000).
[8] C. Liu, Z. Dutton, C. H. Behroozi, and L. V. Hau, Nature (London) **409**, 490 (2001).
[9] D. F. Phillips, A. Fleischhauer, A. Mair, R. L. Walsworth, and M. D. Lukin, Phys. Rev. Lett. **86**, 783 (2001).
[10] A. V. Turukhin, V. S. Sudarshanam, M. S. Shahriar, J. A. Musser, B. S. Ham, and P. R. Hemmer, Phys. Rev. Lett. **88**, 023602 (2002).
[11] J. J. Longdell, E. Fraval, M. J. Sellars, and N. B. Manson, Phys. Rev. Lett. **95**, 063601 (2005).
[12] J. Cheng and S. Han, Phys. Rev. A **76**, 023826 (2007).
[13] K. R. Hansen and K. Mølmer, Phys. Rev. A **75**, 053802 (2007).
[14] A. M. Akulshin, S. Barreiro, and A. Lezama, Phys. Rev. A **57**, 2996 (1998); A. Lezama, A. M. Akulshin, and S. Barreiro, *ibid.* **59**, 4732 (1999).
[15] L. J. Wang, A. Kuzmich, and A. Dogariu, Nature (London) **406**, 277 (2000).
[16] A. M. Akulshin, A. Cimmino, A. I. Sidorov, P. Hannaford, and G. I. Opat, Phys. Rev. A **67**, 011801(R) (2003).
[17] L. Li, H. Guo, F. Xiao, X. Peng, and X. Chen, Phys. Lett. A **327**, 15 (2004).
[18] L. Zhang, Z. Liu, and J. Chen, Sci. China Ser. G **48**, 593 (2005).
[19] A. Joshi and M. Xiao, Phys. Lett. A **317**, 370 (2003).
[20] J. Wen, S. Du, Y. Zhang, M. Xiao, and M. H. Rubin, Phys. Rev. A **77**, 033816 (2008).
[21] D. Han, H. Guo, Y. Bai, and H. Sun, Phys. Lett. A **334**, 243 (2005).
[22] T. N. Dey and G. S. Agarwal, Phys. Rev. A **76**, 015802 (2007).
[23] L. Karpa, F. Vewinger, and M. Weitz, Phys. Rev. Lett. **101**, 170406 (2008).
[24] A. Joshi and M. Xiao, Phys. Rev. A **71**, 041801(R) (2005).
[25] C. Wei, D. Suter, A. S. M. Windsor, and N. B. Manson, Phys. Rev. A **58**, 2310 (1998).
[26] M. Yan, E. G. Rickey, and Y. Zhu, Phys. Rev. A **64**, 013412 (2001).
[27] L. Yang, L. Zhang, X. Li, L. Han, G. Fu, N. B. Manson, D. Suter, and C. Wei, Phys. Rev. A **72**, 053801 (2005).
[28] R.-Y. Chang, W.-C. Fang, Z.-S. He, B.-C. Ke, P.-N. Chen, and C.-C. Tsai, Phys. Rev. A **76**, 053420 (2007).
[29] S. E. Harris and Y. Yammamoto, Phys. Rev. Lett. **81**, 3611 (1998).
[30] C. Y. Ye and A. S. Zibrov, Phys. Rev. A **65**, 023806 (2002).
[31] Y. Rostovtsev, I. Protsenko, and H. Lee, J. Mod. Opt. **49**, 2501 (2002); H. Lee, Y. Rostovtsev, C. J. Bednar, and A. Javan, Appl. Phys. B **76**, 33 (2003).
[32] R. Buffa, S. Cavalieri, E. Sali, and M. V. Tognetti, Phys. Rev. A **76**, 053818 (2007).
[33] H. Lee and M. O. Scully, Found. Phys. **28**, 585 (1998).
[34] E. Arimondo, *Progress in Optics* (Elsevier Science, Amsterdam, 1996), Vol. 35, p. 257.
[35] M. O. Scully and M. S. Zubairy, *Quantum Optics* (Cambridge University Press, Cambridge, UK, 1997).
[36] G. Morigi and E. Arimondo, Phys. Rev. A **75**, 051404(R) (2007).
[37] L.-M. Kuang, Z.-B. Chen, and J.-W. Pan, Phys. Rev. A **76**, 052324 (2007).
[38] D. D. Yavuz and N. A. Proite, Phys. Rev. A **75**, 041802(R) (2007).
[39] F. Zhou, Y. Niu, and S. Gong, J. Chem. Phys. **131**, 034105 (2009).
[40] K. R. Dastidar and S. Dutta, Europhys. Lett. **82**, 54003 (2008).
[41] J. Qi, F. C. Spano, T. Kirova, A. Lazoudis, J. Magnes, L. Li, L. M. Narducci, R. W. Field, and A. M. Lyyra, Phys. Rev. Lett. **88**, 173003 (2002).

[42] L. Li, P. Qi, A. Lazoudis, E. Ahmed, and A. M. Lyyra, Chem. Phys. Lett. **403**, 262 (2005).
[43] E. Ahmed and A. M. Lyyra, Phys. Rev. A **76**, 053407 (2007).
[44] A. Lazoudis, E. Ahmed, L. Li, T. Kirova, P. Qi, A. Hansson, J. Magnes, and A. M. Lyyra, Phys. Rev. A **78**, 043405 (2008).
[45] A. Lazoudis, T. Kirova, P. Qi, E. Ahmed, and A. M. Lyyra, (submitted to Phys. Rev. A).
[46] S. Ghosh, J. E. Sharping, D. G. Ouzounov, and A. L. Gaeta, Phys. Rev. Lett. **94**, 093902 (2005).
[47] P. S. Light, F. Benabid, G. J. Pearce, F. Couny, and D. M. Bird, Appl. Phys. Lett. **94**, 141103 (2009).
[48] H. Chen, H. Li, Y. V. Rostovtsev, M. A. Gubin, V. A. Sautenkov, and M. O. Scully, e-print arXiv:0902.2745v1 [quant-ph].
[49] E. Ahmed, A. Hansson, P. Qi, T. Kirova, A. Lazoudis, S. Kotochigova, A. M. Lyyra, L. Li, J. Qi, and S. Magnier, J. Chem. Phys. **124**, 084308 (2006).
[50] S. J. Sweeney, E. H. Ahmed, P. Qi, T. Kirova, A. M. Lyyra, and J. Huennekens, J. Chem. Phys. **129**, 154303 (2008).
[51] O. Salihoglu, P. Qi, E. Ahmed, S. Kotochigova, S. Magnier, and A. M. Lyyra, J. Chem. Phys. **129**, 174301 (2008).
[52] G. R. Welch, G. G. Padmabandu, E. S. Fry, M. D. Lukin, D. E. Nikonov, F. Sander, M. O. Scully, A. Weis, and F. K. Tittel, Found. Phys. **28**, 621 (1998).
[53] K. Ichimura, K. Yamamoto, and N. Gemma, Phys. Rev. A **58**, 4116 (1998).
[54] D. J. Fulton, S. Shepherd, R. R. Moseley, B. D. Sinclair, and M. H. Dunn, Phys. Rev. A **52**, 2302 (1995).
[55] P. Kusch and M. M. Hessel, J. Chem. Phys. **67**, 586 (1977).
[56] B. Barakat, R. Bacis, F. Carrot, S. Churassy, P. Crozet, F. Martin, and J. Verges, Chem. Phys. **102**, 215 (1986).
[57] E. R. I. Abraham, N. W. M. Ritchie, W. I. McAlexander, and R. G. Hulet, J. Chem. Phys. **103**, 7773 (1995).
[58] K. Urbanski, S. Antonova, A. Yiannopoulou, A. M. Lyyra, L. Li, and W. C. Stwalley, J. Chem. Phys. **104**, 2813 (1996); **116**, 10557(E) (2002).
[59] X. Wang, J. Magnes, A. M. Lyyra, A. J. Ross, F. Martin, P. M. Dove, and R. J. Le Roy, J. Chem. Phys. **117**, 9339 (2002).
[60] R. J. Le Roy, N. S. Dattani, J. A. Coxon, A. J. Ross, P. Crozet, and C. Linton, J. Chem. Phys. **131**, 204309 (2009).
[61] C. R. Vidal and J. Cooper, J. Appl. Phys. **40**, 3370 (1969).
[62] S. Antonova, K. Urbanski, A. M. Lyyra, F. C. Spano, and L. Li, Chem. Phys. Lett. **267**, 158 (1997).
[63] S. Gerstenkorn and P. Luc, *Atlas du Spectre d'Absorption de la Molecule d'Iode* (Editions du CNRS, Paris, 1978).
[64] S. Gerstenkorn and P. Luc, Rev. Phys. Appl. **14**, 791 (1979).
[65] J. Sagle, R. K. Namiotka, and J. Huennekens, J. Phys. B: At. Mol. Opt. Phys. **29**, 2629 (1996).
[66] D. R. Skinner and R. E. Whitcher, J. Phys. E **5**, 237 (1972).
[67] A. E. Siegmann, M. W. Sasnett, and T. F. Johnson, IEEE J. Quantum Electron. **27**, 1098 (1991).
[68] S. Stenholm, *Foundations of Laser Spectroscopy* (Wiley, New York, 1984).
[69] C. L. Bentley Jr. and J. Liu, Opt. Commun. **169**, 289 (1999).
[70] S. H. Autler and C. H. Townes, Phys. Rev. **100**, 703 (1955).
[71] L. M. Narducci (private communication).
[72] J. Qi, Ph.D. thesis, Temple University, 2000.
[73] Y. B. Band and P. S. Julienne, J. Chem. Phys. **97**, 9107 (1992).
[74] F. C. Spano, J. Chem. Phys. **114**, 276 (2001).
[75] Y. B. Band and P. S. Julienne, J. Chem. Phys. **94**, 5291 (1991).
[76] J. Qi, G. Lazarov, X. Wang, L. Li, L. M. Narducci, A. M. Lyyra, and F. C. Spano, Phys. Rev. Lett. **83**, 288 (1999).
[77] R. R. Moseley, S. Shepherd, D. J. Fulton, B. D. Sinclair, and M. H. Dunn, Opt. Commun. **119**, 61 (1995).
[78] S. A. Hopkins, E. Usadi, H. X. Chen, and A. V. Durrant, Opt. Commun. **138**, 185 (1997).
[79] G. Muller, M. Muller, A. Wicht, R.-H. Rinkleff, and K. Danzmann, Phys. Rev. A **56**, 2385 (1997).
[80] J. J. Sakurai, *Advanced Quantum Mechanics* (Addison-Wesley, Reading, MA, 1967, revised 1973).
[81] G. Baumgartner, H. Kornmeier, and W. Preuss, Chem. Phys. Lett. **107**, 13 (1984).
[82] R. J. Le Roy, LEVEL 7.5: A Computer Program for Solving the Radial Schrödinger Equation for Bound and Quasibound Levels, Chemical Physics Research Report No. CP-655, University of Waterloo, 2002.